EXPERIMENTAL AND NUMERICAL STUDY ON PROGRESSIVE FLOODING IN FULL-SCALE

(DOI No: 10.3940/rina.2010.a4.195)

P Ruponen, Napa Ltd, Finland
P Kurvinen, Aalto University School of Science and Technology, Finland
I Saisto, VTT, Finland
J Harras, Finnish Naval Research Institute, Finland

SUMMARY

A series of full-scale flooding tests was performed with a decommissioned fast attack craft. Various flooding scenarios were investigated and the floating position and progress of the floodwater were carefully measured. Also air compression inside a flooded tank was studied. The results were used to validate a state-of-the-art numerical flooding simulation tool. A comprehensive analysis of the experimental and numerical results is presented. A good correlation is found, especially when the applied permeabilities and discharge coefficients are properly selected. Finally, the stability of the flooded ship was studied by comparing the results of an inclining experiment and calculations with the lost buoyancy method.

1. INTRODUCTION

A breach in the hull of the ship, due to a collision or grounding, results in flooding of the damaged compartments. Passenger ships and navy vessels usually have a complex internal subdivision. Thus progressive flooding, even within a single watertight compartment, can result in a dangerous situation due to transient asymmetric flooding. These intermediate phases of flooding can only be assessed with a time-domain approach.

Flooding and damage stability have been studied in numerous model tests throughout the years, for example in [1], [2] and [3], to mention just a few. Recently the increased computing capacity has allowed also detailed numerical analyses, and various time-domain simulation tools for progressive flooding have been developed. The experimental results have been used to validate the calculation methods, for example in the recent ITTC benchmark studies, [4].

Flooding of a real full-scale ship involves factors that are difficult, or even impossible, to take into account in model tests. One of these is the air compression inside a damaged tank with a limited ventilation level. Previously, e.g. Palazzi and de Kat [2] have reported model tests, where also the air compression was included. The problem is that in model scale air is much stiffer and the compression does not follow Froude's scaling law. A depressurized towing tank is one solution for avoiding this problem, but still some full-scale experiments were considered to be necessary in order to get a better insight into the flooding characteristics of a tank with restricted ventilation.

The real permeability of the flooded compartments can differ notably from the model test arrangements, where impermeable blocks are often used to model the large equipment, such as engines, [4]. Also thicker decks and bulkheads are needed in model scale for structural reasons. On the other hand, the stiffeners and small equipment are completely ignored. Also the flow through various openings can be different due to the scale effects.

In order to provide further information on the different flooding mechanisms and to validate a numerical time-domain flooding simulation code, a national research project was carried out in Finland. A decommissioned vessel of the Finnish Navy provided a unique opportunity for the full-scale flooding tests. The experiments were performed by the Finnish Naval Research Institute. VTT (Technical Research Centre of Finland) carried out the measurements while Napa Ltd and Aalto University (former Helsinki University of Technology) were responsible for the planning of the tests, numerical simulations [5] and the final analysis of the results.

In this paper the test arrangement and measurements are presented. The main emphasis is on the comparison of experimental and numerical results.

2. TEST ARRANGEMENT

2.1 FAC TURKU

The vessel that was used in the tests is a decommissioned Fast Attack Craft *Turku* of the Finnish Navy (Figure. 1). The principal dimensions of the vessel are listed in Table 1. The weapon systems had been removed and additional weights were used to compensate this.

Flooding of two watertight compartments was allowed. A butterfly valve with a diameter of 250 mm was installed on the side shell of the starboard side empty tank (Figure. 2), about 1.1 m below the waterline. The valve was opened by a diver in order to let the water flood in. The flooded compartments consist of empty tanks, pump room, equipment room and an empty store. An additional opening was installed on the transverse

bulkhead at frame #25 in order to allow flooding to the store room in the forward compartment. The general arrangement is presented in Figure. 3. Photos of the rooms and openings are shown in Figure. 4 and 5, respectively.

In the numerical model the large tanks in the pump room were taken into account as separate rooms. This ensured that the permeability in this room is properly divided also in the transverse and longitudinal directions. The anti-sloshing bulkheads in the side tanks (Figure. 4a) were included in the numerical model of the ship and each manhole was modelled as a separate opening.

The "damaged" side tank was equipped with two air pipes (diameters 65 mm and 100 mm). This allowed also tests with notable air compression. The other rooms were practically fully ventilated through large openings in the tween deck and ventilation ducts.

Table 1: Main dimensions of the ship

Length over all:	45	m
Maximum breadth:	8.8	m
Displacement:	221	ton
Metacentric height:	1.10	m

Figure 1: Fast Attack Craft *Turku* (photo credit: Finnish Defence Forces)

Figure 2: Butterfly valve used as a damage hole

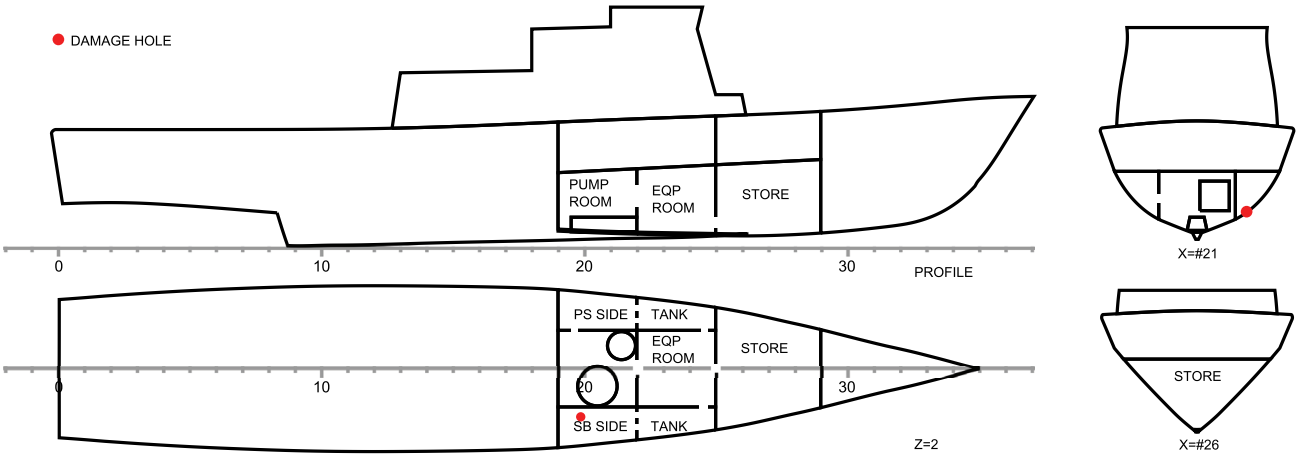

Figure 3: General arrangement of the flooded compartments.

Figure 4: Flooded compartments: a) side tank with anti-sloshing bulkhead, b) equipment room and c) pump room

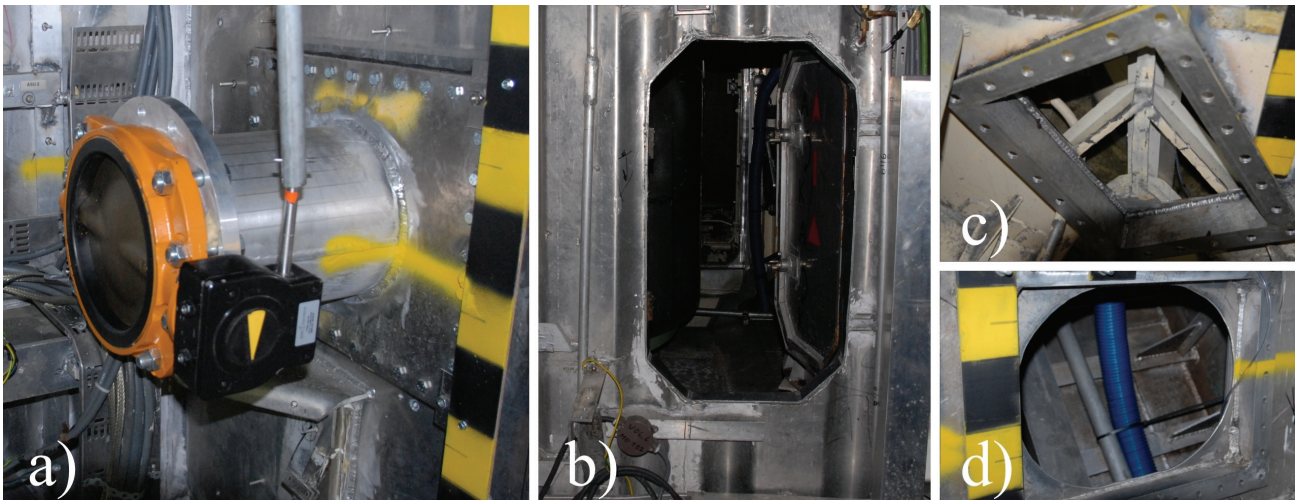

Figure 5: Openings between the flooded rooms: a) valve between the SB side tank and the equipment room, b) open door between the equipment and pump rooms at frame #22, c) the hole in the bulkhead at frame #25 and d) manhole from the equipment room to the PS side tank

2.2 TEST CONDITIONS

The flooding tests were performed in the covered dry dock of STX Europe Helsinki Shipyard in Finland between August 31st and September 3rd 2009. The water level in the dock was calm and there was practically no wind at all. The ship was located a few meters from the side of the dock. The gangway was lifted and the mooring ropes were kept loose in order to avoid any external forces. Thus the environmental conditions were excluded.

During the tests a couple of persons stayed onboard, watching for possible uncontrolled flooding and taking care of the measurement system. In calculations, these additional (moving) masses were considered to be ignorable.

After each test, the damage hole (i.e. the valve) was closed and the flooded water was pumped out (Figure. 6). This arrangement proved to be very successful and only minimal amount of water was left in the bilge. Therefore, each test started from almost identical intact condition. The very small changes in the initial heeling angle were taken into account in the simulations. The powerful pumping equipment allowed fast emptying of the flooded compartments, thus making it possible to do several tests within a short time.

Figure 6: Pumping after a flooding test

2.3 MEASUREMENTS

In order to follow the progress of floodwater in different rooms with local stiffeners and brackets, the floodwater level had to be measured in several locations. The hydrostatic pressure was measured from the bottom of the rooms with 16 differential pressure sensors (Figure. 7). The measured hydrostatic pressure values were used to determine the water levels. In addition air pressure was measured from the top of every flooded room.

The local flow velocities at the damage hole and in the end of the smaller air pipe were also recorded. After the valve (Figure. 2), the flow velocity close to the pipe surface was measured by using a paddle wheel transducer. The airflow velocity was measured with a pitot tube in the centre of the small air pipe from the SB side tank.

The heel and trim angles were measured with MRU 6 motion sensor, which used three axes gyros and linear accelerometers. In addition, the draft marks of the vessel were monitored during the experiments. Environmental conditions, the density of the water and the atmospheric pressure inside the covered dock, were also measured. Furthermore, all flooded rooms were equipped with video cameras in order to allow visual observations of the flooding process.

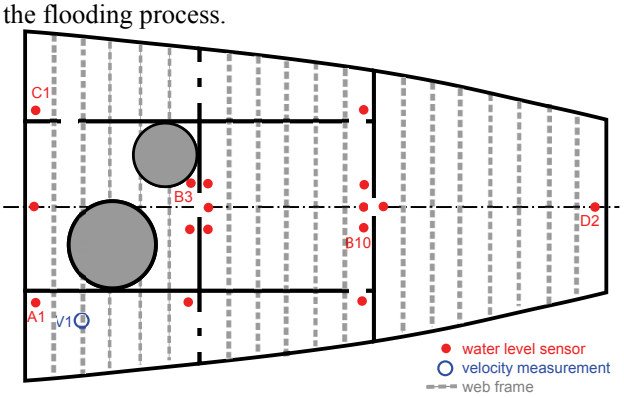

Figure 7: Measurement points

3. NUMERICAL SIMULATIONS

3.1 CALCULATION METHOD

All tested damage cases were calculated with a time-domain flooding simulation tool in the NAPA software. The details of the applied algorithm are described by Ruponen, [6] and [7]. In principle the simulation is based on Bernoulli's equation (conservation of momentum), which is solved simultaneously with the equation of continuity by using a pressure-correction algorithm with implicit time integration. The pressure losses in the openings are taken into account by using semi-empirical discharge coefficients. The following gives a brief introduction to the applied method.

At each time step the conservation of mass must be satisfied in each flooded room. The equation of continuity is:

$$\int_{\Omega} \frac{\partial \rho}{\partial t} d\Omega = -\int_{S} \rho \mathbf{v} \cdot d\mathbf{S} \qquad (1)$$

where ρ is density, t is time, $\mathbf{v}$ is the velocity vector and S is the surface that bounds the control volume Ω. The normal vector of the surface points outwards from the control volume.

The velocities in the openings are calculated by applying Bernoulli's equation for a streamline from point A that is in the middle of a flooded room to point B in the opening:

$$\int_{A}^{B} \frac{dp}{\rho} + \frac{1}{2}\left(u_B^2 - u_A^2\right) + g\left(h_B - h_A\right) + \frac{1}{2} k_L u_B^2 = 0 \qquad (2)$$

where p is air pressure, u is flow velocity and h is the water level height from the common reference level. All losses in the opening are represented by the non-dimensional pressure-loss coefficient k_L. It is assumed that $u_A = 0$. Consequently, the water flow through an opening with area dS is:

$$dQ = C_d \sqrt{2\left[g\left(h_A - h_B\right) + \frac{p_A - p_B}{\rho} \right]} dS \qquad (3)$$

where the discharge coefficient is:

$$C_d = \frac{1}{\sqrt{1 + k_L}} \qquad (4)$$

The calculation within a time step is iterative, based on the linearized Bernoulli's equation, [6] and [7]. The algorithm corrects the hydrostatic and air pressures in the flooded rooms until both Bernoulli's equation for each opening and the conservation of mass for each room is satisfied with sufficient accuracy. This is controlled by the applied convergence criterion. The floating position of the ship is calculated on the basis of the distribution of floodwater in the compartments. The progressive flooding is considered as added weight. In this study, the dynamic roll motion was calculated with the assumption of linear damping. The other degrees-of-freedom (trim and draft) were considered to be quasi-stationary.

The airflows and air pressures are solved by using the approximation of perfect gas and Bernoulli's equation for compressible fluid. Furthermore, the flooding process is considered to be isothermal. All water levels are assumed to be flat and horizontal. The pressure-correction algorithm solves a combination of hydrostatic pressures (water level heights) and air pressures that satisfy both the conservation of mass and momentum (Bernoulli's equation for each opening). This method has proven to be very efficient and numerically stable, even with very complex flooding cases, [8]. Previously this simulation method has been successfully validated against model test experiments, [9].

3.2 INPUT PARAMETERS

The results of a flooding simulation depend on the applied parameters for the openings and the flooded compartments. These are discussed in the following.

3.2 (a) Discharge coefficients

The flow rate through an opening is directly proportional to the applied discharge coefficient, equation (3). Typically in literature, for example [10], a constant discharge coefficient $C_d = 0.6$ is used for all openings. But obviously the flow characteristics can vary significantly since the discharge coefficient depends on the shape and size of the opening.

In this study the results of the full-scale experiments within the FP7 European Union funded research project FLOODSTAND, [11], were used. For manholes, the rough estimation corresponds rather well with the measurements for free discharge into air. However, when the discharge was into water, somewhat larger values (up to 0.70) were obtained in the full-scale tests for a manhole, [11].

Special attention was paid to the two (almost identical) valves since they included a short pipe. After the flooding tests, one valve was removed and extensively tested in the flume of the Water Engineering Group of the Aalto University School of Science and Technology. Most notably, different values were eventually used for these valves due to the completely different flow conditions. The "damage hole" valve is submerged very rapidly and discharges to water with a large pressure head most of the flooding process. The valve that is located between the side tank and the equipment room discharges to air with a small pressure head for a very long time. This is taken into account by applying a smaller discharge coefficient. On the other hand, when

this valve is fully submerged a larger coefficient is needed. The different flow conditions are illustrated in the video captures in Figure. 8. Consequently, two separate values are used for this opening, depending whether the discharge is to water (C_d = 0.70) or to air (C_d = 0.41). All the applied discharge coefficients are listed in Table 2.

Figure 8: Different flow conditions of the valve between the side tank and the equipment room

Table 2: Applied discharge coefficients for water flow

Opening:	*Rough estimation*	*Detailed analysis*
damage hole	0.60	0.78
valve side tank/eqp room	0.60	0.41 & 0.70
manholes	0.60	0.68
open door	0.60	0.70
hole eqp room/store	0.60	0.60

3.2 (b) Permeability

The applied permeabilities are usually taken from the SOLAS regulations without any further analysis. However, a variable permeability is sometimes used in vertical direction in order to model the fact that most of the equipment is not usually evenly distributed.

The large tanks in the pump room were modelled as separate rooms and thus the permeability of the remaining part was increased to compensate this. The direct modelling of large impermeable equipment provides a realistic distribution of the permeability, also in transverse and longitudinal directions. All the loose objects and also the insulation were removed before the tests. Especially, the store room was practically empty (Figure. 9), and thus a very large permeability was used. All the applied permeabilities are listed in Table 3.


Figure 9: Empty store in the forward compartment

Table 3: Applied permeabilities

Room	*SOLAS*	*Rough estimation*	*Detailed analysis*
side tanks	0.95	0.95	0.95
equipment room	0.85	0.90	0.94
pump room	0.85	0.85	0.90
store	0.60	0.95	0.97

3.3 PERFORMED SIMULATIONS

The hull form in the numerical model was created on the basis of a laser scanning. Before the tests, the floating position of the ship was checked from the draft marks. In addition the weight of the ship was measured after the tests when she was lifted from the dock. Based on these measurements, the displacement, draft and trim could be determined. The ship had a small initial heeling to port side. The centre of gravity was determined by performing an inclining test with all the necessary measurement and pumping equipment installed onboard. These data determined the initial condition for the simulations.

The quality of the numerical results depends on the accuracy and reliability of the applied input data. In the case of flooding simulation, the precise values of the permeabilities and discharge coefficients are not usually known. Furthermore, these parameters are always based on some simplifications. In order to study the effect of the input data, simulations were also performed with rough estimations for discharge coefficients (C_d = 0.6) and permeabilities.

Constant time step of 0.1 s was used for the flooding case with restricted ventilation (section 4.1) and 0.2 s for the cases with slow progressive flooding. The applied convergence criterion corresponds to a water height difference of 0.01 mm. It was checked that neither a shorter time step nor a stricter criterion had any notable influence on the results.

Trim and vertical motion (sinkage) were considered to be quasi-stationary but the roll motion of the ship was calculated by assuming linear damping (ξ = 0.1) and a rough estimation for the natural roll period ($T_\phi \approx$ 15 s).

The time that it took to open the “damage hole” valve (typically about 5 s) is taken into account in the simulations by linearly increasing the effective area of the opening.

3.4 CO-ORDINATE SYSTEM

All calculations were done with the NAPA software, using a co-ordinate system, where heeling towards the damaged side (SB) is negative and bow trim is positive. The water level heights are presented as the vertical distance between the horizontal water level and the measurement point.

4. VALIDATION OF THE SIMULATION METHOD

4.1 FLOODING OF A SIDE TANK

In this test the ventilation level of the flooded side tank was restricted. The diameter of the air pipe is 65 mm and the pipe length is approximately 2.5 m, including several bends (Figure. 10). The larger air pipe was closed in this test. Thus the air pipe size is less than 7 % of the damage hole area. This is much smaller than required in the IMO Resolution MSC.245(83) [12] for assumption of full ventilation in a cross-flooding calculation. The discharge coefficient for the airflow in the pipe was estimated by using the formulae in the Appendix of the IMO Resolution MSC.245(83), resulting in $C_{d,air} = 0.62$.

The measured and calculated heeling angles are presented in Figure. 11 Air overpressure and water level in the flooded side tank are presented in Figure. 12 and 13, respectively. There was no notable change in the trim angle. The simulation with the rough estimations results in too slow flooding. Also the peak of the air pressure is under-estimated.

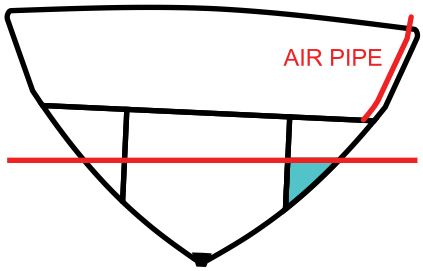

Figure 10: Flooded side tank with the small air pipe

With more realistic input data the correspondence to the measurements is much better. However, especially the air overpressure in the tank is equalized slightly later than measured.

In comparison of measured and calculated water levels, some difference can be noticed in the start of the flooding. This is explained by the fact that the stiffeners and brackets in the bottom of the tank (Figure. 4a) delayed the progress of floodwater inside the tank and resulted in more rapid change of the water level at the sensor location.

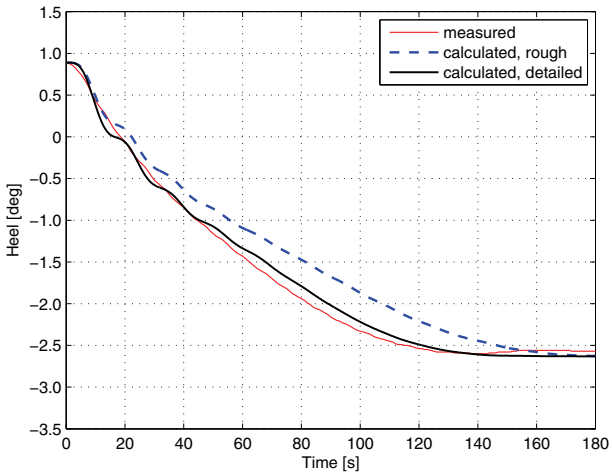

Figure 11: Heel angle for side tank flooding

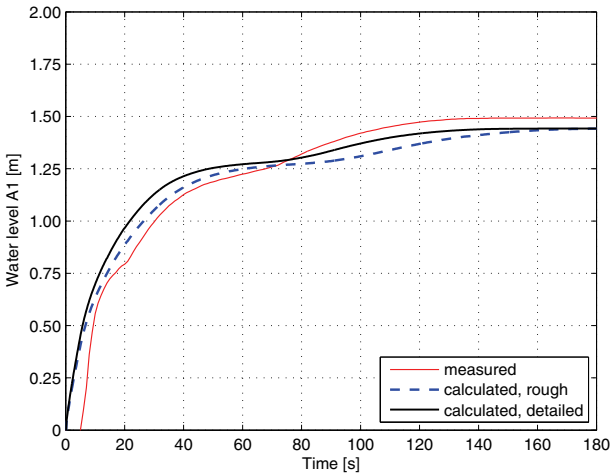

Figure 12: Water level in the flooded side tank

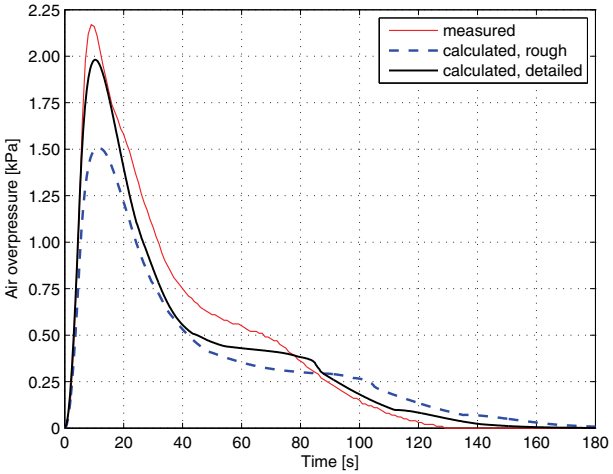

Figure 13: Air overpressure for side tank flooding

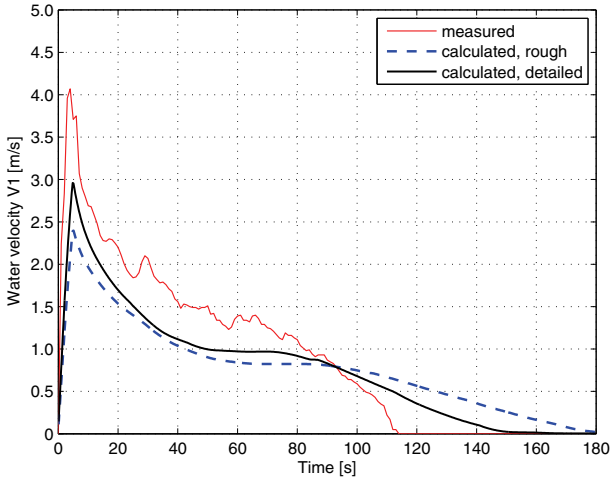

Figure 14: Flow velocity in the damage opening for the side tank flooding

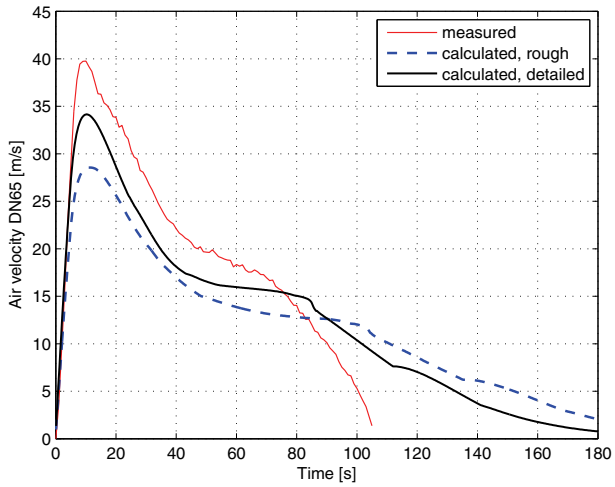

Figure 15: Airflow velocity in the air pipe for the side tank flooding

The measured and calculated flow velocities in the "damage hole" valve are presented in Figure. 14. The measurement did not succeed at small velocities, and consequently the flow seems to stop too early. However, the general correspondence with the simulation is good.

The measured air flow velocity in the centre of the air pipe is shown in Figure. 15. It is noteworthy that the maximum flow velocity is almost 40 m/s, even through the damage size is small and the maximum overpressure is only 2.0 kPa. Similarly to the water flow measurement, the flow seems to stop too early. This is caused by the unreliability of the applied pitot tube with small flow velocities. The presented simulation results are average velocities in the pipe cross-section, and thus they are not fully comparable with the measurement.

4.2 ONE-COMPARTMENT FLOODING

In this test the side tank with the damage hole was first flooded and then water proceeded to the equipment room through an open valve that was installed in the longitudinal bulkhead (Figure. 5a). The progressive flooding then continued to the pump room through an open door with a high sill (Figure. 5b). In the final phase of the flooding the water progressed from the pump and equipment rooms to the empty tank in the intact side (PS) of the ship through two open manholes (Figure. 5d). Both air pipes in the damaged tank were open and no notable air compression was observed in any of the flooded rooms. Thus all the rooms were modelled as fully vented in the simulation. The final calculated floating position is shown in Figure. 16.

The time histories for measured and calculated heel and trim angles are presented in Figure. 17 and 18, respectively. Contrary to the side tank flooding case, the rough estimations for the discharge coefficients result in too fast flooding. This is explained by the large pressure losses in the valve between the side tank and the equipment room. The dedicated hydraulic tests of the valve in the flume at Aalto University confirmed that the effective discharge coefficient is much smaller than the rough estimation (C_d = 0.60) when the flow discharges to air with a small pressure head.

The trim angle is slightly over-estimated in the simulations, especially in the early stages. This results from the observed fact that water first accumulated between the stiffeners. This was not taken into account in the numerical model. Thus in the simulations water immediately accumulated to the forward part of the room due to the bow trim.

The sudden increase of the heel angle at $t \approx 900$ s is under-estimated by the simulation. At this time the flooding of the pump room starts. Therefore, the likely explanation for the difference is that water is accumulated between the structures on the damaged side of the pump room.

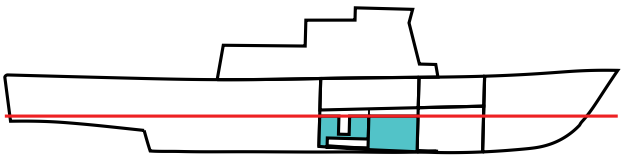

Figure 16: One-compartment flooding case

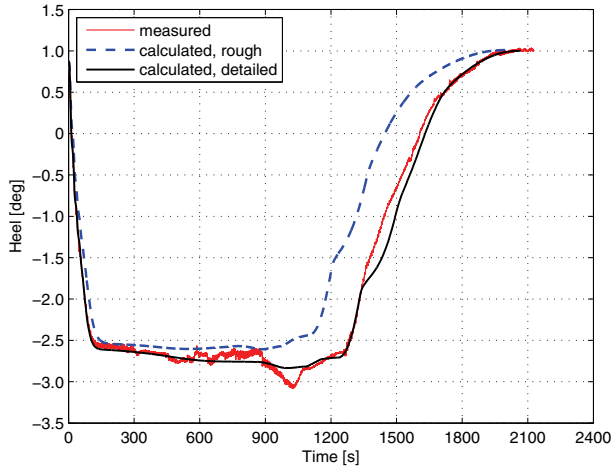

Figure 17: Heel angle for one-compartment flooding

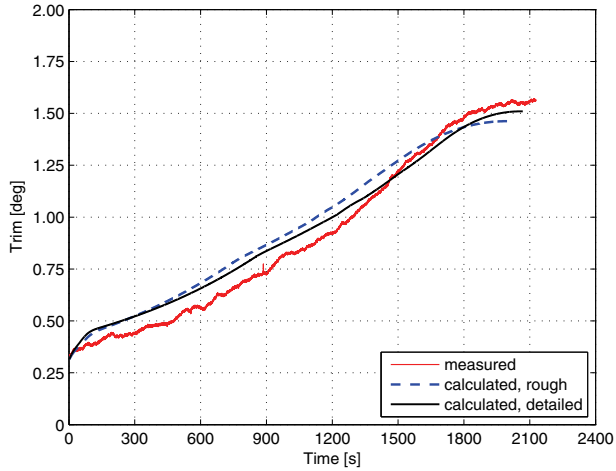

Figure 18: Trim angle for one-compartment flooding

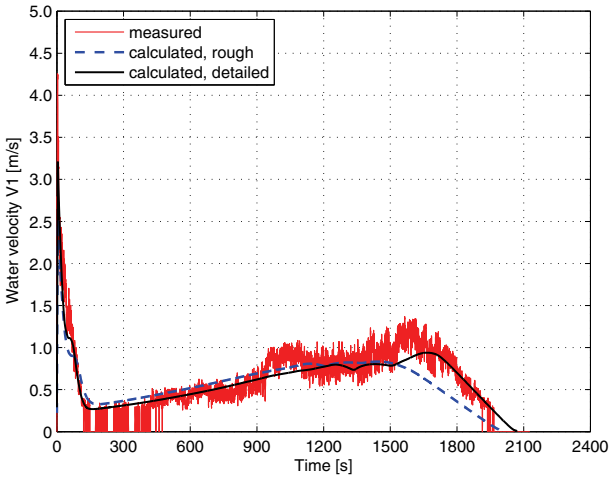

Figure 19: Flow velocity in the damage opening for one-compartment flooding

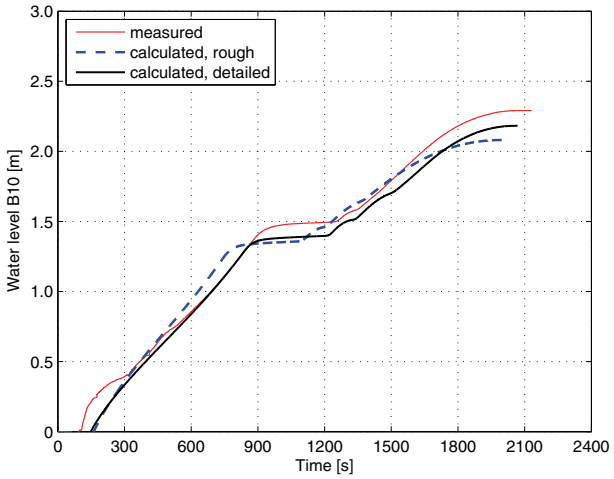

Figure 20: Water level in the equipment room for one-compartment flooding

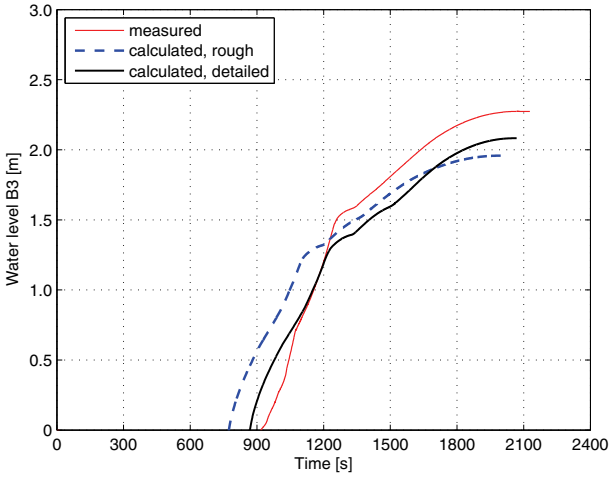

Figure 21: Water level in the pump room for one-compartment flooding

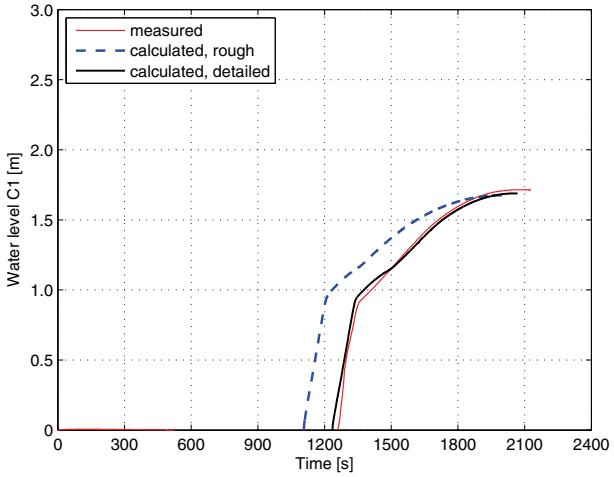

Figure 22: Water level in the PS side tank for one-compartment flooding

The flow velocity in the "damage hole" valve is presented in Figure. 19. Very small velocities ($V < 0.3$ m/s) could not be measured properly. Furthermore, there is quite a lot of noise in the signal. However, the general correspondence between the measurement and the calculation with detailed input data is good.

Water levels in the equipment room, pump room and PS side tank are presented in Figure. 20, 21 and 22, respectively. The final calculated values for equipment and pump rooms are slightly lower than in the measurements. This may be caused by an inaccuracy in the modelled locations of the water level sensors. This explanation is supported by the notice that the water levels are lower in the calculations than in the measurements at periods, where the increase of water level has momentarily stopped when floodwater has progressed to the next room. The water level in the PS tank is predicted very well by the simulation with the detailed input data.

4.3 TWO-COMPARTMENT FLOODING

An additional opening was installed in the bottom of the transverse watertight bulkhead between the equipment room and the store (Figure. 5c). In this test the opening was left open to allow flooding of the store. Similarly to the previous cases, the empty SB side tank was flooded first. Then water progressed to the equipment room through the open valve (Figure. 5a), and further to the store and later also to the pump room through the open door (Figure. 5b). The port side tank was empty and closed during this test, thus causing a notable heeling also at the end.

The openings from the equipment room to the store and to the pump room were large, when compared to the size of the damage hole. Consequently the water levels in these three rooms increased practically simultaneously. The calculated final floating position is illustrated in Figure. 23 and captures from a stationary camera are presented in Figure. 24, showing the initial and final conditions.

This flooding case had to be stopped just before the final equilibrium condition in order to avoid uncontrolled flooding of the tween deck. This was done by closing the valve in the longitudinal bulkhead between the SB side tank and equipment room. The simulations were continued until the final equilibrium.

An empty small tank in the pump room was also flooded through an open connection near the top of the room. Also this was taken into account in the numerical model.

Both air pipes in the damaged tank were open and no notable air compression was observed during the test. Thus in simulation all rooms were modelled to be fully vented.

The measured and calculated results for heel and trim are shown in Figure. 25 and 26. Interestingly, the use of rough estimations for the discharge coefficients seems to provide a better correspondence with the measured heel angle.

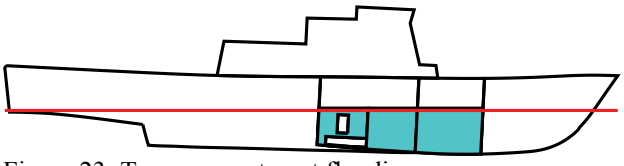

Figure 23: Two-compartment flooding case

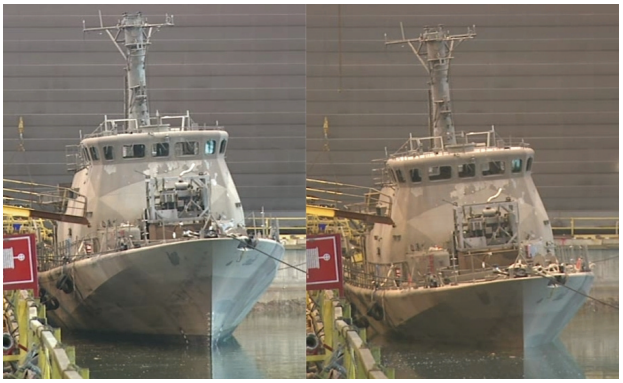

Figure 24: Initial and final condition after two-compartment flooding from a stationary camera

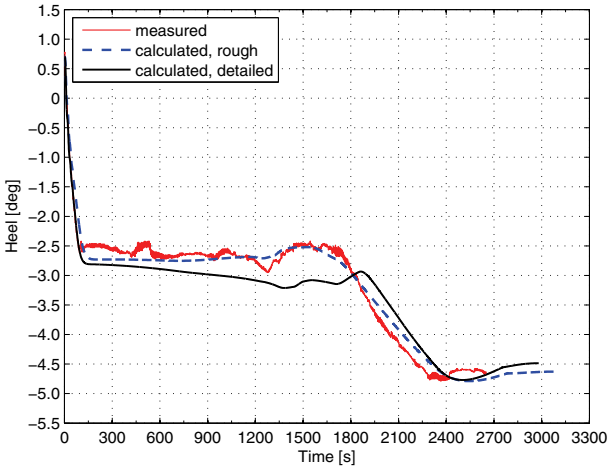

Figure 25: Heel angle for two-compartment flooding case

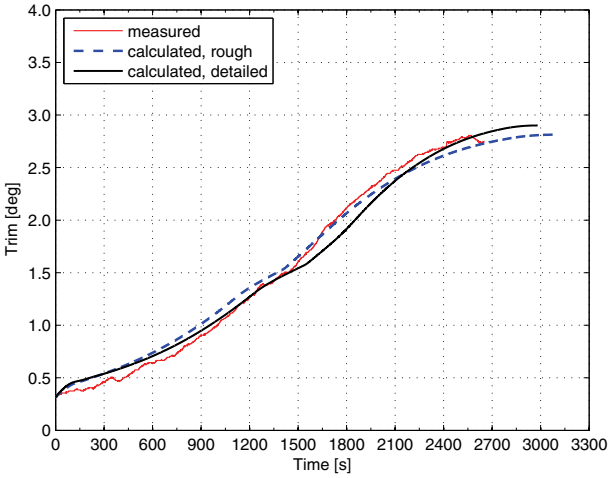

Figure 26: Trim angle for two-compartment flooding Case

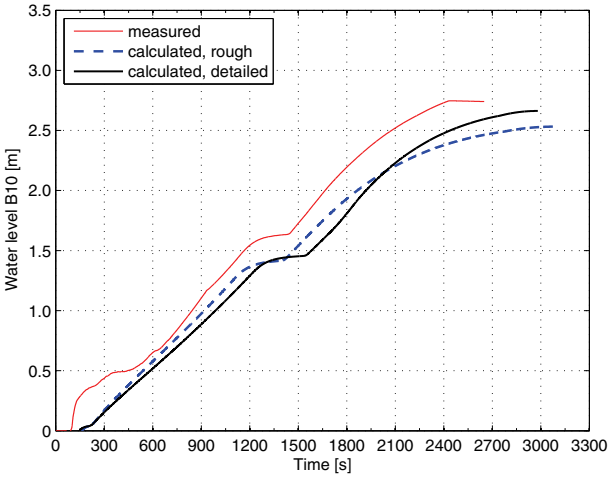

Figure 27: Water level in the equipment room for two-compartment flooding case

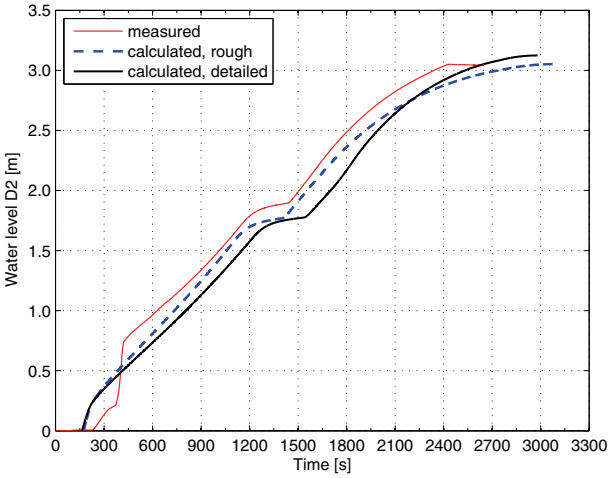

Figure 28: Water level in the forward end of the store for two-compartment flooding case

The time histories for water levels in the equipment room and the store are presented in Figure. 27 and 28. The notable differences between the measurement and the calculations in the early stages are caused by the water accumulation between the stiffeners in the bottom of the rooms. The numerical model does not contain these structural details. Thus the floodwater is calculated to accumulate on the forward end of the empty store in the beginning of the flooding, resulting in a slight over-estimation of both the trim and heel angles. This effect is slightly compensated by the slower flooding with the rough estimations for the input data. However, the overall correspondence between the measurements and the simulation is good.

4.4 STABILITY AFTER FLOODING

After the test with the side tank flooding, an inclining experiment was conducted, using movable weights on the upper deck. The damage hole was left open. The righting lever curve for the final condition after the flooding was calculated with the NAPA software. The lost buoyancy method was used.

The results are presented in Figure. 29. The measurement points fit very well in the calculated curve. The difference in the metacentric height is less than 0.01 m, which is clearly within the accuracy limits of the measurement.

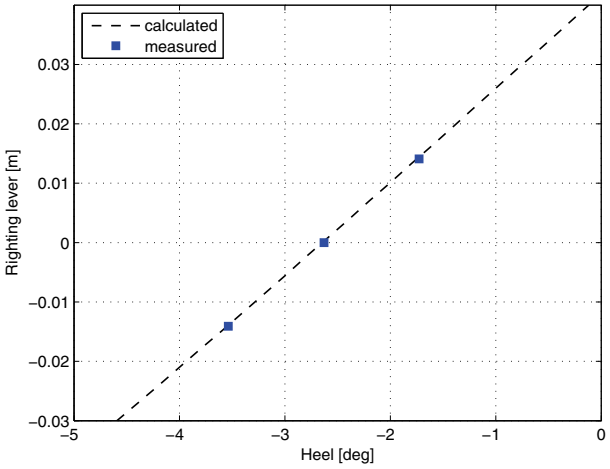

Figure 29: Calculated righting lever curve and measurements from the inclining test with flooded side tank

5. CONCLUSIONS

Although large ships have been intentionally sunk in order to establish artificial reefs and diving attractions, [13], systematic experimental research on progressive flooding in full-scale has not been reported in open literature. Contrary to the artificial reef projects, the presented full-scale tests allowed detailed measurements and recordings inside the flooded compartments. Moreover, the experiments could be easily repeated.

The applied test arrangement proved to be very successful. Flooding was well-controlled and the "damage hole" could be easily closed. Therefore, several tests could be performed within a short time. On the other hand the damage size was small, resulting in fairly slow flooding. The ship had a relatively good initial stability, and thus the maximum heeling angle was rather small, even in an asymmetric flooding case. Yet the changes in the floating position were significant, especially in the two-compartments flooding case.

Comprehensive measurements and video recordings were used to validate a state-of-the-art flooding simulation tool. The calculation predicts very well the progress of the floodwater and the motions of the ship, even with very rough estimations of the permeabilities and the pressure losses in the openings.

When real permeabilities and proper discharge coefficients are applied, the results match even better. Taking into account the above mentioned uncertainties in the modelling of the discharge coefficients, and especially the permeabilites and structural details, it can be concluded that the correspondence between the numerical simulation results and the measurements is as good as in the validation study with a scale model of a box-shaped barge, [9].

It should be noted that in the presented tests the damage hole was rather small. Thus the effect of its discharge coefficient is much more notable than in the case of a large damage extent. Furthermore, the valve between the SB side tank and the equipment room acts as a bottleneck since the effective pressure head is rather low throughout the flooding process. Consequently the simulation results are sensitive to the applied discharge coefficient for this opening.

The comparison of experiments and simulations clearly shows that the simplified approach of Bernoulli's theorem is accurate enough for modelling progressive flooding inside a damaged ship, if the applied discharge coefficients are realistic. Furthermore, the air compression in a tank with restricted ventilation level can be modelled very realistically with the assumption of perfect gas and Bernoulli's equation for compressible fluid.

6. ACKNOWLEDGEMENTS

The authors would like to express their sincere gratitude to all persons who were involved in the flooding tests. The project has received funding from Tekes (the Finnish Funding Agency for Technology and Innovation) and STX Europe Turku Shipyard, which is gratefully acknowledged. Mikael Stening from Water Resources Laboratory of Aalto University provided the valuable data on pressure losses in various openings. Finally, Turkka Jäppinen from Finnish Naval Research Institute is thanked for arranging the opportunity for the tests.

7. REFERENCES

1. BIRD, H., BROWNE R.P. Damage Stability Model Experiments, *Transactions of RINA, Vol. 116, pp. 69-91*, 1974.
2. PALAZZI, L., DE KAT, J. Model Experiments and Simulations of a Damaged Ship with Air-Flow Taken into Account, *Marine Technology, Vol. 41, pp. 38-44*, 2004.
3. CHO, SK., SUNG, HG., NAM, BW., HONG, SY., KIM, KS. Experimental Study on Flooding of a Cruiser in Waves, *Proceedings of the 10th International Conference on Stability of Ships and Ocean Vehicles STAB2009*, St. Petersburg, Russia 22-26.6.2009, pp. 747-753, 2009.
4. ITTC. The Specialist Committee on Stability in Waves, Final Report and Recommendations, Proceedings of the 25th ITTC, Vol. II, pp. 605-639, 2008.
5. KURVINEN, P. Flooding of a Naval Vessel, Master's Thesis, Aalto University School of Science and Technology, 2010.
6. RUPONEN, P. Pressure-Correction Method for Simulation of Progressive Flooding and Internal Airflows, *Ship Technology Research – Schiffstechnik, Vol. 53, pp. 63-73*, 2006.
7. RUPONEN, P. Progressive Flooding of a Damaged Passenger Ship, Dissertation for the degree of Doctor of Science in Technology, Helsinki University of Technology, *TKK Dissertations 94*, 2007.
8. RUPONEN, P. On the Application of Pressure-Correction Method for Simulation of Progressive Flooding, *Proceedings of the 10th International Conference on Stability of Ships and Ocean Vehicles STAB2009*, St. Petersburg, Russia 22-26.6.2009, pp. 271-279, 2009.
9. RUPONEN, P., SUNDELL, T., LARMELA, M. Validation of a Simulation Method for Progressive Flooding, *International Shipbuilding Progress, Vol. 54, pp 305-321* (first presented in STAB2006), 2007.
10. VASSALOS, D., TURAN, O., PAWLOWSKI, M. Dynamic Stability Assessment of Damaged Passenger/Ro-Ro Ships and Proposal of Rational Survival Criteria, *Marine Technology, Vol. 34, No. 4, pp. 241-266*, 1997.
11. STENING M. Pressure Losses and Flow Velocities in Flow through Manholes and Cross-Ducts, *FLOODSTAND Deliverable D2.3*, Aalto University, School of Science and Technology, 18 May 2010.
12. IMO Resolution MSC.245(83) Recommendation on a Standard Method for Evaluating Cross-Flooding Arrangements, adopted 12 October 2007.
13. HYNES, M.V., PETERS, J.E., RUSHWORTH, D. Artificial Reefs – A Disposal Option for Navy and MARAD Ships, *RAND National Defense Research Institute,* 2004.